HHS Public Access

Author manuscript

ACS Appl Mater Interfaces. Author manuscript; available in PMC 2020 September 09.

Published in final edited form as:

ACS Appl Mater Interfaces. 2017 January 25; 9(3): 2169–2180. doi:10.1021/acsami.6b15009.

Low Initial Modulus Biodegradable Polyurethane Elastomers for Soft Tissue Regeneration

Cancan Xu[†,‡], **Yihui Huang**[†,‡], **Liping Tang**[†,‡], **Yi Hong**[†,‡,*]

[†]Department of Bioengineering, University of Texas at Arlington, Arlington, TX 76019, USA

[‡]Joint Biomedical Engineering Program, University of Texas Southwestern Medical Center, Dallas, TX 75093, USA

Abstract

The mechanical match between synthetic scaffold and host tissue remains challenging in tissue regeneration. The elastic soft tissues exhibit low initial moduli with a J-shaped tensile curve. The suitable synthetic polymer scaffolds requires low initial modulus and elasticity. To achieve these requirements, random copolymers polyδ-valerolactone-cε-caprolactone) (PVCL) and hydrophilic poly(ethylene glycol) (PEG) were combined into a triblock copolymer PVCL-PEG-PVCL, which was used as a soft segment to synthesize a family of biodegradable elastomeric polyurethanes with low initial moduli. The triblock copolymers were varied in chemical components, molecular weights and hydrophilicities. The mechanical properties of polyurethanes in dry and wet states can be tuned by altering the molecular weights and hydrophilicities of the soft segments. Increasing the length of either PVCL or PEG in the soft segments reduced initial moduli of the polyurethane films and scaffolds in dry and wet states. The polymer films are found to have good cell compatibility and to support fibroblast growth *in vitro*. Selected polyurethanes were processed into porous scaffolds using thermally induced phase separation technique. The scaffold from PU-PEG_{1K}-$PVCL_{6K}$ had an initial modulus of 0.60±0.14 MPa, which is comparable with the initial modulus of human myocardium (0.02-0.50MPa). The *in vivo* mouse subcutaneous implantation of the porous scaffolds showed minimal chronic inflammatory response and intensive cell infiltration, which indicated the good tissue compatibility of the scaffolds. The biodegradable polyurethane elastomers with low initial modulus and good biocompatibility and processability would be an attractive alternative scaffold material for soft tissue regeneration, especially for heart muscle.

Graphical Abstract

[*]**Corresponding author:** Yi Hong, yihong@uta.edu, Tel: +1-817-272-0562; Fax: +1-817-272-2251.

Author Contributions

Y.H. designed the research. C.X. conducted experiments and data analysis. YH.H and L.T. evaluated *in vivo* biocompatibility of the scaffolds. C.X. and Y.H. wrote and edited the manuscript. All authors reviewed the paper.

Supporting Information

Cyclic stretching curves of porous scaffolds at 30% deformation in dry and wet states. This material is available free of charge via the Internet at http://pubs.acs.org.

The authors declare no competing financial interest.

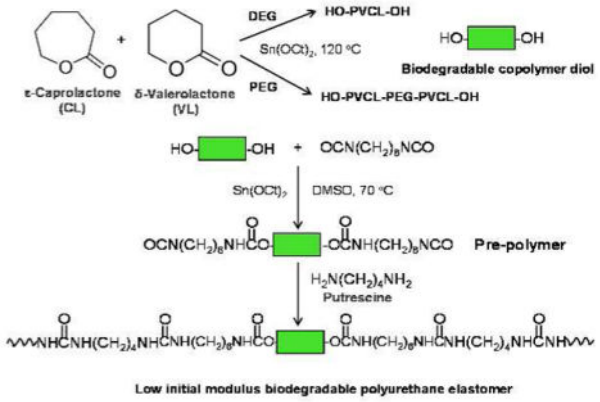

Keywords

mechanical match; initial modulus; polyurethane; biodegradable; porous scaffold; soft tissue engineering

INTRODUCTION

Mechanically matched scaffolds are essential for tissue engineering and regeneration.[1] Specifically, repairing different host tissues requires biodegradable scaffolds with distinct biomechanics, such as load bearing, force generation, and transmission.[2] The mechanical mismatch between the scaffolds and host tissues would trigger foreign body reactions and/or cause implantation failure. For example, the mechanical mismatch between rigid implants and soft brain tissue would stimulate neuro inflammatory response.[3] The mechanical mismatch between vascular graft and human artery would result in intimal hyperplasia and thrombosis.[4] The mechanical mismatch between the synthetic cardiac patch and the host myocardium would lead to abnormal cardiac functions, such as arrhythmia.[5] Generally, most of the soft elastic tissues showed a typical J-shaped stress-strain curve with relatively low elastic moduli, such as 0.1–2 MPa for skin,[6] 0.002–0.1 MPa for aortic valve leaflet,[7, 8] and 0.02–0.5 MPa for heart muscle.[9, 10] Therefore, it is crucial to develop low initial modulus biodegradable elastomers for soft tissue regeneration.

Biodegradable polyurethanes are very attractive for promoting soft tissue regeneration because of their good biocompatibility, and strong and elastic mechanical properties similar to the soft tissues. Variety of biodegradable polyurethanes have been investigated to repair soft tissues, such as abdominal wall,[11] heart and blood vessels,[12-14] adipose,[15] and skin.[16] Soft segment, hard segment, and chain extender are generally used to synthesize segmented polyurethanes. The mechanical properties of polyurethanes can be flexibly tuned by altering these three blocks.[17-19] For example, a biodegradable polyurethane from poly(δ-valerolactone-cε-caprolactone) (PVCL, molecular weight = 6000) diol soft segment and 1,4-diisocyanatobutane (BDI) hard segment with putrescine chain extender had an initial modulus of 2.8±1.3MPa (film) in dry state, which has markedly lower initial modulus than a polyurethane (12.1±2.5 MPa) based on the semicrystalline polycaprolatone (PCL), BDI and putrescine.[17] However, the value still is higher than those of soft tissues. To further decrease

the initial moduli of polyurethanes under a physiological condition, one promising strategy is to incorporate hydrophilic PEG into the soft segment.[20] The incorporation of PEG can markedly enhance the water absorption ability of polymers.[21] The absorbed water in "bound state" can attach to polymer chains via hydrogen bonding and work as a plasticizer, which can reduce initial modulus.[22, 23]

In this study, we synthesized a series of biodegradable elastic polyurethanes with low initial moduli using a novel soft segment, which can be used to engineer the low-moduli soft elastic scaffold to mechanically match with soft tissues. We firstly synthesized new triblock copolymer of PVCL-PEG-PVCL with different PEG molecular weights and total molecular weights, where the PVCL block is random with VL/CL molar ratio of 50/50 to maximally reduce crystallinity. The polyurethanes were then synthesized using three major components, the new complex triblock PVCL-PEG-PVCL as a soft segment, hexamethylene diisocyanate (HDI) as a hard segment and putrescine chain extender. The polyurethanes synthesized from copolymer PVCL diols without PEG block were set as controls. The chemical structure, thermal properties, *in vitro* degradation, and cell compatibility of polyurethane films were investigated. The mechanical properties were tested in dry and wet states. The selected polyurethane scaffolds were prepared by thermally induced phase separation (TIPS) and then characterized mechanically in dry and wet states. Mouse subcutaneous implantation was utilized to evaluate *in vivo* tissue compatibility and cell infiltration ability of the scaffolds to verify their potential applications for soft tissue engineering. .

MATERIALS AND METHODS

Materials

All chemicals were obtained from Sigma unless otherwise noted. δ-Valerolactone (VL), HDI and putrescine were distilled before synthesis. The residual water was removed for diethylene glycol (DEG) in a vacuum oven at 60°C. Caprolactone (CL), PEG (MW=1000 and 2000), stannous octoate ($Sn(Oct)_2$), diethyl ether, anhydrous dimethyl sulfoxide (DMSO), dichloromethane (DCM), 1,1,1,3,3,3-hexafluroisopropanol (HFIP, Oakwood Product), hexamethyldisilazane (HMDS) and lipase from *Thermomyceslanuginosus* (≥100,000 U/g) were used as received.

Synthesis of PVCL copolymer diols and PVCL-PEG-PVCL triblock copolymer diols

The random copolymer PVCL and triblock copolymer PVCL-PEG-PVCL diols were obtained using VL and CL by ring-opening polymerization using $Sn(Oct)_2$ as a catalyst and DEG (for PVCL synthesis) or PEG (molecular weight=1000 and 2000) as an initiator (Figure 1A), respectively.[17, 24] VL, CL and DEG or PEG were mixed in a flask (250 mL), and reacted at 120°C under N_2 protection with $Sn(Oct)_2$. After 24h, the synthesized polymer diols were dissolved in dichloromethane, and then precipitated in cold diethyl ether. The obtained polymer diols were dried at 60°C for 3 days in a vacuum oven for further polyurethane synthesis. The molar ratio of VL/CL was fixed as 50/50.

Synthesis of polyurethanes

The polyurethanes (PUs) were synthesized from PVCL or PVCL-PEG-PVCL diols, HDI and putrescine via a two-step solution polymerization (Figure 1B).[25] Polymer diols and HDI with $Sn(Oct)_2$ were reacted in DMSO at 70°C in a glass flask with N_2 input and stirring for 3 h, The putrescine/DMSO mixture was then added into the prepolymer solution at room temperature. After 18 h, the polymer was precipitated using deionized water, and purified in isopropanol. The obtained polymer was vacuum dried at 60°C for 2 d. The molar ratio of polymer diol/HDI/putrescine was set as 1:2:1. The yields of all products were above 90%. The synthesized polyurethanes were named as PU-PEG_x-$PVCL_y$, where x and y denote the molecular weight of PEG and PVCL, respectively. Polyurethane films were prepared using solvent casting method. The solvent is HFIP. The obtained films were further dried at 60 °C in a vacuum oven for 3 days.[26]

Polymer characterization

The chemical structure and relative component molecular weight of PVCL and PVCL-PEG-PVCL diols were characterized by ^1H nuclear magnetic resonance (^1H-NMR, JEOL ECX 300 MHz) using CD_3Cl as a solvent. The block length of the copolymer diols can be calculated through the NMR spectra by the integrals of specific peaks from DEG or PEG segments and those from PVCL segments. Fourier transform infrared spectrometer (FTIR, Nicolet 6700, Thermo Electron Corporation) was used to verify chemical structures of polyurethanes.

Differential scanning calorimetry (DSC-60, Shimazu) was used to characterize the film thermal properties from −100 to 200 °C with 10°C/min heating rate and nitrogen flow. A sessile drop method was utilized to measure water contact angle on the film surface (n=8) in air on a contact angle instrument (FTA-1000B, First Ten Angstroms). For water absorption, the weighed PU films (W_0, n=3) were immersed in phosphate buffer solution (PBS) at 37°C. After 24h, the samples were weighed (W_1) after removing the surface residual water. The water absorption ratio was computed as $(W_1\text{-}W_0)/W_0\times100\%$.

Inherent viscosity (IV) of the polyurethanes was measured using an Ubbelohde viscometer for polymer molecular weight characterization because polyurethanes may damage GPC columns for their strong hydrogen bonding.[27] Each polymer solution (0.1g/dL) in HFIP was filtered using a 1.2 μm glass fiber membrane. The measurement was conducted at 25°C and repeated 5 times. The IV was calculated using $\ln(t_p/t_s)/C_p$. The t_p is the time of polyurethane solution flowing through the glass capillary, the t_s is the time for HFIP solvent alone, and C_p is the concentration of the polyurethane solution.

Uniaxial mechanical properties

The 2×20 mm stripes (n=6) were cut from the PU films, and were tested on a MTS Insight Testing System (500N loading cell) with a 10mm/min cross head rate at room temperature. The measured samples were in both dry and wet states. The instant strain recovery (n=3) was measured by stretching the stripe at 10% strain and 10 mm/min stretching rate, holding for 1 min, and then releasing for 3 times. The instant strain recovery was computed using a formula of $(1\text{-}(L_1\text{-}L_0)/L_0)\times100\%$, where L_0 is the original length of the stripe and L_1 is the

final length after 3 cycles. The cyclic stretch testing was conducted by stretching the stripes (2×20 mm, n=3) to the strain at 30% or 300%, and then released back to 0% strain[17]. This measurement was repeated for 10 cycles at a fixed rate of 10 mm/min.

In vitro degradation

The weighed polymer films (W_0) were immersed in PBS (10 mL, hydrolytic degradation) or 100 U/mL lipase/PBS solution (2 mL, enzymatic degradation) at 37°C.[28] The lipase/PBS solution was refreshed every 3 days. Samples (n=3 for each sample at each time point) were, weighed (W_1) after deionized water rinse and lyophilization. The mass remaining was calculated as $W_1/W_0 \times 100\%$.

In vitro cytocompatibility of polyurethane films

Polyurethane disk (6 mm diameter) were obtained from the films using standard biopsy punches (6mm, Miltex). UV irradiation (1 h, 30 min for each side) was used to sterilize the disks. Before cell seeding, the sterilized disks were rinsed 3 times using sterilized PBS solution and then immersed in DMEM cell culture medium supplemented with 10% fetal bovine serum, 100 U/mL penicillin, and 100μg/mL streptomycin for 24 h. 2×10^3 mouse 3T3 fibroblasts (ATCC, Manassas, VA) were seeded on each disk surface. The cell culture medium was changed every 3 d. A mitochondrial activity assay (MTT) was used to detect the cell metabolic activity (n=5) at days 1, 3 and 5. The 3T3 fibroblast seeded films were fixed using 2.5% glutaraldehyde solution at 4 °C to observe cell morphology. The samples were then dehydrated using a series of ethanol solutions, immersed in HMDS, and dried in the air. The 3T3 fibroblast morphology on the films was recorded under a scanning electronic microscope (SEM, Hitachi S-4800 HRSEM).

Porous scaffold fabrication

The polyurethane scaffolds were fabricated using TIPS according to previous study.[29] A 5% (w/v) polymer solution in DMSO was poured into a glass cylinder mold at 80°C. The mold was then immediately placed in an −80°C freezer. After 3 h, the mold was immersed in 70% ethanol bath at 4°C for 3 d to completely remove DMSO. The scaffold removed from the mold was then immersed in a large amount of deionized water to extract ethanol. The porous scaffold was frozen and lyophilized for further measurements.

Scaffold characterization

The scaffold morphology was observed under SEM, and the pore size was measured using ImageJ (National Institutes of Health, US). The scaffold porosity was tested by ethanol displacement.[30, 31] The mechanical properties of the porous scaffolds were measured using the same protocols as for the polymer films at room temperature. For the suture retention strength, porous scaffolds were cut into 5×20 mm stripes. A loop of 4-0 silk braided suture (Ethicon, Inc.) was formed at 5 mm from one stripe end. Samples were then tested on the MTS Insight Testing System (500 N load cell) with 10 mm/min stretching rate (n=4 for each group). The suture retention strength is obtained using load force (N)/ (suture diameter [mm] × sample thickness [mm]).[32]

Mouse subcutaneous implantation

All experimental designs for animal study were reviewed and approved by the University of Texas at Arlington Animal Care and Use Committee (IACUC) according to the NIH guidelines for the use of laboratory animals. Female Balb/c mice (20–25 grams; Taconic Farms, Germantown, NY) were used. Disk-shaped scaffolds (6 mm diameter by 300 μm thickness, two implants per animal) were placed in the mouse dorsal subcutaneous area. After 2 weeks, the implants and the surrounding tissues were explanted for cryosection and hematoxylin-eosin (H&E) staining. The extent of inflammatory cell recruitment and infiltration around and in the implants was then calculated using ImageJ software.

Statistical analysis

All results exhibited as mean ± standard deviation. One-way ANOVA with a post hoc Tukey-Kramer test was used for all data analysis. For polyurethane film degradation, a repeated measure ANOVA was conducted with the Statistics Analysis System (SAS). Significant difference were considered when $p < 0.05$.

RESULTS

Synthesis and characterization of PVCL and PVCL-PEG-PVCL diols

The ^{1}H-NMR spectra confirmed the chemical structure of synthesized PVCL copolymer diols (Figure 2A) and PVCL-PEG-PVCL triblock copolymer diols (Figure 2B). The specific peaks of methyl protons of the PVCL blocks (in the region between 1.34 to 4.06 ppm in Figure 2A and 2B) were demonstrated in both PVCL and PVCL-PEG-PVCL copolymer diols. The ethylene oxide protons of the PEG block in PVCL-PEG-PVCL triblock copolymer diols were assigned to chemical shifts of 3.66 ppm, 4.35 ppm and 4.23 ppm (Figure 2B). The block lengths of PVCL and PVCL-PEG-PVCL in calculation were close to those in theory. Specifically, the calculated block molecular weight of $PVCL_{2K}$ and $PVCL_{6k}$ were 1936 and 5576, respectively. The theoretical molecular weights of PVCL blocks ranged from 500 to 3000 in PVCL-PEG-PVCL triblock copolymer diols, which were practically distributed as 493-1000-493 in PEG_{1K}-VCL_{1K}, 2763-1000-2763 in PE_{1K}-VCL_{6K}, and 2873-2000-2873 in PEG_{2K}-VCL_{6K} (Table 1).

Synthesis and characterization of polyurethanes

In FTIR spectra (Figure 3), the soft segments in polyurethanes are mainly related to the asymmetrical and symmetrical stretching of the methyl and methylene groups between 2800 and 3000 cm^{-1}. The hard segments in polyurethanes are primarily characterized by the absorption peaks from urethane groups: 3300-3500 cm^{-1} (N-H stretching), 1730 cm^{-1} (C=O stretching), 1530-1580 cm^{-1} (C-N stretching and N-H symmetrical bending). The intensity ratio of hard segment absorption peaks at 3300–3500 cm^{-1} to soft segment absorption peaks at 2800-3000 cm^{-1} can reflect the content ratio of hard segments to soft segments in polymers. Polyurethanes with higher soft segment molecular weight and lower hard segment content showed lower absorption peaks at 3300–3500 cm^{-1}. The peak at 1100 cm^{-1} was mainly assigned to the ether groups of soft segments, and also corresponded to the C-O-C stretching absorptions from urethane groups.[33] The intensities of the C-O-C stretching

absorption peak at 1100 cm^{-1} in PU-$PVCL_{2K}$ and PU-$PVCL_{6K}$ were relatively lower than those in polyurethanes containing PEG segments with abundant ether groups.

All polyurethanes showed low glass transition temperatures (Tgs) (<−55°C) (Table 2). The Tg decreased with soft segment molecular weight increase. Through the comparison between the polyurethanes (PU-$PVCL_{6K}$, PU-PEG_{1K}-$PVCL_{6K}$, and PU-PEG_{2K}-$PVCL_{6K}$) with the same PVCL block molecular weight and various PEG molecular weights, it is apparent that the introduction of PEG segment decreased the Tg. All the polymers showed melting temperatures (Tms) below room temperature from −7°C to 9°C, suggesting that none of the polyurethanes had crystalline domains at room or body temperature. Polymer inherent viscosities ranged from 1.42 to 2.17 dL/g (Table 2).

The surface and bulk hydrophilicity of polyurethane films were characterized by water contact angle and water absorption (Table 2), respectively. The decrease of PVCL block length and the increase of PEG block length in soft segments increased surface hydrophilicity of polyurethanes, which was related to the decreasing water contact angle (p<0.05). The water absorption decreased with increasing PVCL molecular weight (p<0.05). The incorporation of the PEG component into the backbone improved the hydrophilicity of polyurethanes, which was associated with an increase of water absorption (p<0.05). The increasing PEG content in the soft segments from 14 % (PU-PEG_{1K}-$PVCL_{6K}$) to 50 % (PU-PEG_{1K}-$PVCL_{1K}$) resulted in the increase of water absorption from 23±3% (PU-PEG_{1K}-$PVCL_{6K}$) to 65±5% (PU-PEG_{1K}-$PVCL_{1K}$).

Mechanical properties of polymer films

Mechanical properties and typical stress-strain curves of polyurethane films were showed in Table 2 and Figure 4, respectively. In dry state, the tensile strengths of the polyurethane films ranged from 1.1±0.2 to 14.4±1.8 MPa while the initial moduli increased from 2.2±0.3 to 18.6±0.7 MPa, and the breaking strains increased from 296±59 to 1629±249%. The initial modulus and mechanical strength markedly decreased with increased soft segment molecular weight (p<0.05). The PU-PEG_{2K}-$PVCL_{6K}$ with the highest soft segment molecular weight showed the lowest initial modulus (2.2±0.3 MPa) and tensile strength (1.1±0.2 MPa) in dry state. The instant recovery for all polyurethane films was ≥99%.

The introduction of PEG block into soft segments had great effects on the mechanical properties of polyurethanes in wet state, compared to those polyurethanes in dry state (Table 2). For the polyurethanes incorporated with PEG segments (PU-PEG_{1K}-$PVCL_{1K}$, PU-PEG_{1K}-$PVCL_{6K}$, and PU-PEG_{2K}-$PVCL_{6K}$), the initial modulus and tensile stress reduced greatly from dry state to wet state (p<0.05). The initial modulus of PU-PEG_{1K}-$PVCL_{6K}$ decreased from 3.5±0.4 to 2.3±0.6MPa, and its tensile strength decreased from 6.4±0.4 to 4.3±0.3 MPa. However, for the PU-$PVCL_{2K}$ and PU-$PVCL_{6K}$ without PEG segment in the backbone, the mechanical properties did not show significant difference between the dry and wet states (p>0.05). We observed no significant difference on the breaking strain between the dry and wet states, with or without PEG segments (p>0.05).

To further evaluate the polyurethane elasticity, the cyclic stretching was executed with a fixed strain of 30% and 300% in dry and wet states (Figure 5). A large hysteresis loop in the

first cycle was seen for most of the polymers, and then smaller hysteresis loops were shown in the next nine cycles. For a 30% maximum strain, most of the samples exhibited small irreversible deformations (~5%) (Figure 5A-5D, and 5a-5d), except for the PU-PEG_{2K}-$PVCL_{6K}$ (10%-15%) (Figure 5E and 5e). When the strain reached 300%, the permanent deformations became apparent (50%-100%) (Figure 5F-5I, and 5f-5i). The cyclic stretching curves of the PU-PEG_{2K}-$PVCL_{6K}$ film were not obtained at 300% deformation in dry and wet states because of its low breaking strain (296±59% in dry state and 244±35% in wet state).

In vitro degradation of polyurethane films

The degradation property of polyurethane films was measured *in vitro* with or without the presence of 100 U/mL lipase/PBS solutions at 37 °C (Figure 6). The hydrolysis rate of polyurethane films (in PBS alone) markedly increased with increased PEG molecular weight in soft segments and decreased PVCL block length (Figure 6A; $p<0.05$). The PU-$PVCL_{6K}$ showed the lowest degradation rate of 93.8±1.3% mass remaining at 8 weeks, whereas the PU-PEG_{1K}-$PVCL_{1K}$ had the highest degradation rate (75.5±1.3% mass remaining at 8 weeks; $p<0.05$).

For enzymatic degradation in lipase/PBS solution (Figure 6B), the polyurethanes without PEG segments showed markedly higher degradation rates compared to the hydrolytic degradation. During a period of 14 d, the degradation amounts of PU-VCL_{2K} and PU-VCL_{6K} reached 85.8±2.4% and 96.8±1.6%. For the polyurethanes incorporated with PEG block in soft segments, small degradation amounts were observed after 14 d of enzymatic degradation. The degradation amounts of PU-PEG_{1K}-$PVCL_{1K}$, PU-PEG_{1K}-$PVCL_{6K}$, and PU-PEG_{2K}-$PVCL_{6K}$ within 14 d of degradation in lipase/PBS solution were only 5.7±0.4%, 16.8±2.3% and 11.2±1.3%, respectively, which were much smaller than those of PU-VCL_{2K} (85.8±2.4%) and PU-VCL_{6K} (96.8±1.6%) ($p<0.05$).

In vitro cytocompatibility of polyurethane films

The cell compatibility of PU-PEG-VCL films was evaluated by measuring the mouse 3T3 fibroblast survival on the material surfaces for up to 5 days (Figure 7). The cell viability increased on both TCPS and polymer films from day 1 to 5 ($p<0.05$). No significant difference was found between TCPS and polymer films within 5 d culture ($p>0,05$), except for the PU-PEG_{1K}-$PVCL_{1K}$ films that showed fewer cell numbers than other films ($p<0.05$) at 1, 3 and 5 d. The cell numbers on PU-PEG_{2K}-$PVCL_{6K}$ were higher than PU-PEG_{1K}-$PVCL_{1K}$but lower than PU-VCL_{2K} and TCPS at 3 and 5 d ($p<0.05$). The electron micrographs (Figure 7B) of 3T3 fibroblasts seeded on polyurethane films at day 5 were taken to qualitatively confirm the cell proliferation measured by the MTT method. In addition, 3T3 fibroblasts on most of the polyurethane films had a high cell density and formed a confluent cell monolayer, except for the PU-PEG_{1K}-$PVCL_{1K}$.

Porous scaffold characterization

The cross-sectional morphologies of porous scaffolds prepared by TIPS were shown in Figure 8A-8C. The interconnected porous structure was observed. The pore sizes of porous scaffolds ranged from 58±34 to 64±39 μm with porosities above 90% (Table 3).

Typical tensile stress-strain curves of PU-VCL_{6K}, PU-PEG_{1K}-$PVCL_{6K}$ and PU-PEG_{2K}-$PVCL_{6K}$ were shown in Figure 8D and 8E. The tensile strengths and initial moduli of porous scaffolds increased from 0.42±0.05 (PU-PEG_{2K}-$PVCL_{6K}$) to 2.13±0.20 MPa (PU-$PVCL_{6K}$) and 1.19±0.33 (PU-PEG_{2K}-$PVCL_{6K}$) to 3.14±0.52 MPa (PU-$PVCL_{6K}$) in dry state, respectively, with the decrease of soft segment molecular weight (Table 3). After immersion in PBS for 24 h, both of the tensile strengths and initial moduli of PU-PEG_{1K}-$PVCL_{6K}$ and PU-PEG_{2K}-$PVCL_{6K}$ scaffolds decreased markedly (Table 3). The tensile strengths of PU-PEG_{1K}-$PVCL_{6K}$ and PU-PEG_{2K}-$PVCL_{6K}$ scaffolds decreased from 1.08±0.16 MPa and 0.42±0.05 MPa in dry state to 0.31±0.03 MPa and 0.07±0.01MPa in wet state, and the initial moduli of those decreased from 1.91±0.13 MPa and 1.19±0.33 MPa in dry state to 0.60±0.14 MPa and 0.19±0.08 MPa in wet state, respectively. The mechanical properties of PU-$PVCL_{6K}$ scaffold in wet state (tensile strength: 2.50±0.36 MPa and initial modulus: 3.47±0.24 MPa) showed no significant difference with those in dry state (tensile strength: 2.13±0.20 MPa and initial modulus: 3.14±0.52 MPa). There is no significant difference among instant recoveries for all polyurethane scaffolds (p>0.05).

All the scaffolds had one larger hysteresis loop, and then 9 smaller hysteresis loops with a maximum stain at 30% (Figure S1). All three scaffolds had low irreversible deformations (~10%) in dry state (Figure S1A-S1C). However, in wet state, only the PU-$PVCL_{6K}$ showed a modest irreversible deformation (~5%) (Figure S1D). The irreversible deformations of PU-PEG_{1K}-$PVCL_{6K}$ and PU-PEG_{2K}-$PVCL_{6K}$ were at around 15% (Figure S1E and S1F).

Mouse subcutaneous implantation of scaffolds

To investigate *in vivo* cell penetration and tissue compatibility, PU-$PVCL_{6K}$, PU-PEG_{1K}-VCL_{6K}, and PU-PEG_{2K}-VCL_{6K} scaffolds were implanted for 2 weeks. The implant and surrounding tissues were sectioned and H&E stained. H&E images showed minimal inflammatory cells (granulocytes) accumulated at the implant sites (Figure 9A). In addition, obvious cell infiltration and cell attachment surrounding and inside all tested materials were observed (Figure 9A). The number of infiltrating cells in PU-PEG_{1K}-VCL_{6K} (189±8.8) was higher than that in PU-$PVCL_{6K}$ (142±8.5) and PU-PEG_{2K}-VCL_{6K} (132±6.9) (p<0.05) (Figure 9B). We also noticed that the degradation rate of PU-PEG_{2K}-VCL_{6K} was faster than those of the other two materials. The results from the animal study demonstrated that PU-$PVCL_{6K}$, PU-PEG_{1K}-VCL_{6K}, and PU-PEG_{2K}-VCL_{6K} scaffolds have good tissue compatibility and also facilitate cell infiltration.

DISCUSSION

Biodegradable polyurethanes using the soft segments of polyesters[13, 17, 19, 20] or polycarbonates[17, 26, 34] exhibit robust mechanical properties and high elasticity. To achieve the desired properties of polyurethanes, altering segmented components, especially the soft segments in polyurethane, is a relatively easy and efficient approach.[35] In previous studies, a variety of macrodiols have been used as the single component in soft segment, such as PCL,[25, 36] polylactide (PLA),[37] poly(hydrobutyrate) (PHB)[38] and poly(1,3-trimethylene carbonate) (PTMC).[17] To further control the mechanical behavior and degradation profile of polyurethanes, copolymer diols have been developed for the soft segment in polyurethane

backbone, such as PCL-co-PVL,[17] PCL-PEG-PCL,[20, 39] poly(ethylene oxide)–poly(propylene oxide)–poly(ethylene oxide) (PEO-PPO-PEO),[35] and PTMC-PEO-PPO-PEO-PTMC.[34] To obtain polyurethanes with lower initial moduli, we designed a new triblock copolymer diol (PVCL-PEG-PVCL) as the soft segment in polyurethanes, including random copolymer PVCL block and hydrophilic segment PEG. Our results support that the mechanical properties of polyurethanes can be manipulated through changing their chemical components, molecular weights and hydrophilicities of the soft segments.

PCL, PVL and PEG (MW=1000, 2000) showed Tgs lower than −60°C.[17, 40] The low Tgs of the polyurethanes (below −55°C) were mainly dependent on the composition of their soft segments. The Tgs of the polyurethanes decreased with increasing PEG contents in soft segments, which was attributed to the lower Tg of PEG (−79°C and −76°C for PEG1000 and PEG2000, respectively) than PCL (−63°C) and PVL (−72°C).[17, 40] The low Tms of the polyurethanes (−7 to 9°C) were mainly attributed to the soft segment crystallinity. The random polymerization of VL and CL increased the irregular arrangement of polymer chains, and subsequently reduced the polymer crystallization. When the molar ratio of CL to VL was 50/50, the polymer chain structure reached the maximum randomness, which maximally reduced crystalline compared to the semicrystalline PCL (Tm=61°C).[17]

The mechanical properties of the synthesized polyurethanes can be adjusted through altering the molecular weights and hydrophilicities of the soft segments in polyurethane backbone to meet the mechanical requirements of the variable native soft tissues. The ability to decrease initial modulus and tensile strength by increasing molecular weight of soft segments (Table 2) is in consistent with the rubber thermodynamic theory. The theory claims that the initial modulus of an elastomeric polymer increases with the decrease of its average molecular weight between cross-link points.[17, 41] Incorporation of PEG into the soft segments greatly decreased the tensile strength and initial modulus of the polyurethanes in wet state (Table 2) due to the hydrophilicity of PEG. After the polymers were immersed in the water, the water molecules penetrated into the polymer and attached to the hydrophilic groups on polymer chains, and then the hydrogen bonds were established between water and polymer. The bound water contribute to the polymer plasticization, thus decreasing the mechanical strength and modulus of polymer.[23, 42] The synthesized polyurethanes showed good elasticity with low permanent deformations (<10%) at a maximum strain of 30%. When the strain reached 300%, all the hard segment domains were reorganized to form permanent deformations, which resulted in a large deformation of all polyurethanes (50%–100%). The polyurethane porous scaffolds showed consistent results with the polyurethane films, but the mechanical strength decreased due to the porous structure.[43] The developed polyurethane porous scaffolds possessed attractive low initial modulus for soft tissue scaffolds. For example, the initial modulus of PU-PEG_{1K}-$PVCL_{6K}$ (0.60±0.14 MPa) in wet state is comparable with that of native human heart muscle (0.02–0.50 MPa).[9] The initial moduli of PU-PEG_{1K}-$PVCL_{6K}$ (0.60±0.14 MPa) and PU-PEG_{2K}-$PVCL_{6K}$ (0.19±0.08 MPa) in wet state are similar with that of skin (0.1-2.0 MPa).[6]

The hydrolytic degradation in PBS for the polyurethanes was influenced by both the hydrophilic PEG block and hydrophobic and degradable polyester block of PVCL in the polyurethane backbone. The higher mass loss of polyurethanes was associated with

increased PEG molecular weight and decreased PVCL block length. The ester bonds which mainly existed in the PVCL segment were considered as the initial cleavage position in poly(ester urethane)s during the hydrolysis.[44] The PEG segment that allowed the high penetration of water molecules into the polyurethane matrix structure could lead to a high hydrolysis rate.[44] The trend of polyurethane degradation behavior suggests that the greater water penetration and access to the labile ester bonds is more important than the density of ester bonds in the PVCL segments, which is consistent with the previous report.[20] The enzymatic degradations of the polyurethanes in lipase solution were faster than those in PBS, which was attributed to the ester bond sensitive to the lipase.[13, 45] The degradation rate of the polyurethanes without PEG content (PU-VCL_{2K} and PU-VCL_{6K}) in lipase solution was higher compared with the polyurethanes containing PEG segment (PU-PEG_{1K}-$PVCL_{1K}$, PU-PEG_{1K}-$PVCL_{6K}$, and PU-PEG_{2K}-$PVCL_{6K}$). Two main reasons may lead to this phenomenon. Firstly, the hydrolase lipase is used as the catalyst of ester-bond cleavage with hydrolysis,[13, 45] whereas the ether bond is not as sensitive to the lipase as the ester bond. The polyester based polyurethanes were reported to be more sensitive to fungal degradation compared with the polyether based polyurethanes.[46] Secondly, the surface hydrophobicity of polymer was reported to be beneficial to the protein adsorption,[47, 48] further accelerating the polymer enzymatic degradation which occurred preferentially on the polymer surface.[46] In terms of the water contact angles of the polyurethanes (Table 2), introducing PEG segments into the polyurethane backbone led to an increase of polymer surface hydrophilicity. Improved hydrophilicity would reduce protein adsorption, which might compromise the polyurethane enzymatic degradation. This phenomenon was also found for the degradation of poly(ether urethane) in a polyester hydrolase of cholesterol esterase (CE) .[49] Only a small loss in polyurethane films was observed after 36 days of enzymatic degradation in CE. Therefore, the involvement of PEG segment in the polyurethane backbone can promote the polymer hydrolysis but cannot accelerate the enzymatic degradation of the polyurethanes.

The synthesized polyurethanes exhibited good cytocompatibility and tissue compatibility via *in vitro* and *in vivo* assessments. The chemical components in the polyurethane, including PCL, PVL, PEG, and HDI, have been used in FDA-approved devices.[25] These ensure the good biocompatibility of the polyurethanes. The lower cell viability on PU-PEG_{1K}-$PVCL_{1K}$ film compared with TCPS and other groups ($p<0.05$) was primarily due to its high hydrophilicity. It may decrease protein adsorption onto the hydrophilic polyurethanes and induce less cell adhesion.[20] Many studies have proven the good *in vivo* biocompatibility of polyurethane scaffolds.[25, 26, 50] The good long-term tissue compatibility of a polyurethane from poly(DL-lactide/ε-caprolactone), BDI, and butanediol was concluded by a 3-year *in vivo* subcutaneous implantation study in both rat and rabbit.[50] Polyurethane scaffolds based on poly(ester carbonate urethane)urea (PECUU) and polyurethanes with disulfide bonds (PU-SS) also had good tissue response in rat and mouse subcutaneous models after 8-week implantation, respectively.[25, 26] Similar with above biodegradable polyurethanes, the *in vivo* mouse subcutaneous implantation (2 weeks) showed PU-$PVCL_{6K}$, PU-PEG_{1K}-VCL_{6K}, and PU-PEG_{2K}-VCL_{6K} scaffolds have good tissue compatibility with good cell infiltration, which indicated that the polyurethane scaffolds could be safely used as biodegradable implants.

Some limitations in this study should be mentioned. First, although the mechanical testing has confirmed the low initial moduli of the new polymers and scaffolds, other mechanical testing, such as biaxial mechanical testing and ball burst testing,[51, 52] can be used to further evaluate the polyurethane scaffold biomechanics under physiological conditions in the future. Second, the scaffold mechanical properties were manipulated by altering polymer types. The mechanical properties of the polyurethane scaffolds fabricated using TIPS can also be optimized by varying other parameters, such as polymer concentration and quenching temperature.[29, 53, 54] Third, the 2-week examination period of subcutaneous implantations is common to initially evaluate the scaffold short-term immune response and cell infiltration. But it can be further extended to investigate the *in vivo* degradation of the scaffolds, and their long-term tissue response.

CONCLUSION

A family of copolymer diols was synthesized from PVCL and PEG as soft segments of biodegradable polyurethanes. The mechanical properties of these degradable polyurethanes can be tailored simply by altering the molecular weight and hydrophilicity of the copolymer diols. These new polyurethane elastomers showed strong and flexible mechanical properties with low initial moduli. Further, the polymers were processed into porous scaffolds with comparable initial moduli to the soft tissues. The polymer films and porous scaffolds showed good cellular compatibility *in vitro* and tissue compatibility *in vivo*. These biodegradable polyurethanes would have the potential for soft tissues repair and regeneration.

Supplementary Material

Refer to Web version on PubMed Central for supplementary material.

ACKNOWLEDGMENT

We greatly appreciate the supports from the Research Enhancement Program of the University of Texas at Arlington, the Beginning Grant-in-Aid #14BGIA20510066 from the American Heart Association and the CAREER award #1554835 from the National Science Foundation, and the grant #R56NS095046 from National Institutes of Health.

REFERENCES

(1). Butler DL; Goldstein SA; Guilak F Functional Tissue Engineering: the Role of Biomechanics. J. Biomech. Eng 2000, 122, 570–575. [PubMed: 11192376]

(2). Guilak F; Butler DL; Goldstein SA; Baaijens FP Biomechanics and Mechanobiology in Functional Tissue Engineering. J. Biomech 2014, 47, 1933–1940. [PubMed: 24818797]

(3). Nguyen JK; Park DJ; Skousen JL; Hess-Dunning AE; Tyler DJ; Rowan SJ; Weder C; Capadona JR Mechanically-Compliant Intracortical Implants Reduce the Neuroinflammatory Response. J. Neural Eng 2014, 11, 056014. [PubMed: 25125443]

(4). Stewart SF; Lyman DJ Effects of a Vascular Graft/Natural Artery Compliance Mismatch on Pulsatile Flow. J. Biomech 1992, 25, 297–310. [PubMed: 1564063]

(5). Xu B; Li Y; Fang X; Thouas GA; Cook WD; Newgreen DF; Chen Q Mechanically Tissue-Like Elastomeric Polymers and Their Potential as a Vehicle to Deliver Functional Cardiomyocytes. J. Mech. Behav. Biomed. Mater 2013, 28, 354–365. [PubMed: 24125905]

(6). Holzapfel GA In The Handbook of Materials Behavior Models; Lemaitre J, Ed.; Academic: Boston, MA, 2001; pp 1049–1063.

(7). Hasan A; Ragaert K; Swieszkowski W; Selimović S; Paul A; Camci-Unal G; Mofrad MR; Khademhosseini A Biomechanical Properties of Native and Tissue Engineered Heart Valve Constructs. J. Biomech 2014, 47, 1949–1963. [PubMed: 24290137]

(8). Christie G Anatomy of Aortic Heart Valve Leaflets: the Influence of Glutaraldehyde Fixation on Function. Eur. J. Cardio-Thorac. Surg 1992, 6, S25–S33.

(9). Chen QZ; Bismarck A; Hansen U; Junaid S; Tran MQ; Harding S. n. E.; Ali NN; Boccaccini AR Characterization of a Soft Elastomer Poly(glycerol sebacate) Designed to Match the Mechanical Properties of Myocardial Tissue. Biomaterials 2008, 29, 47–57. [PubMed: 17915309]

(10). Weis SM; Emery JL; Becker KD; McBride DJ; Omens JH; McCulloch AD Myocardial Mechanics and Collagen Structure in the Osteogenesis Imperfecta Murine (oim). Circ. Res. 2000, 87, 663–669. [PubMed: 11029401]

(11). Hong Y; Takanari K; Amoroso NJ; Hashizume R; Brennan-Pierce EP; Freund JM; Badylak SF; Wagner WR An Elastomeric Patch Electrospun from a Blended Solution of Dermal Extracellular Matrix and Biodegradable Polyurethane for Rat Abdominal Wall Repair. Tissue Eng. Part C Methods 2012, 18, 122–132. [PubMed: 21933017]

(12). Xu Y; Patnaik S; Guo X; Li Z; Lo W; Butler R; Claude A; Liu Z; Zhang G; Liao J Cardiac Differentiation of Cardiosphere-Derived Cells in Scaffolds Mimicking Morphology of the Cardiac Extracellular Matrix. Acta Biomater. 2014, 10, 3449–3462. [PubMed: 24769114]

(13). Fang J; Ye S-H; Wang J; Zhao T; Mo X; Wagner WR Thiol Click Modification of Cyclic Disulfide Containing Biodegradable Polyurethane Urea Elastomers. Biomacromolecules 2015, 16, 1622–1633. [PubMed: 25891476]

(14). Silvestri A; Sartori S; Boffito M; Mattu C; Rienzo AM; Boccafoschi F; Ciardelli G Biomimetic Myocardial Patches Fabricated with Poly(ε-caprolactone) and Polyethylene Glycol-Based Polyurethanes. J. Biomed. Mater. Res. B Appl. Biomater 2014, 102, 1002–1013. [PubMed: 24307433]

(15). Wittmann K; Storck K; Muhr C; Mayer H; Regn S; Staudenmaier R; Wiese H; Maier G; Bauer-Kreisel P; Blunk T Development of Volume-Stable Adipose Tissue Constructs Using Polycaprolactone-Based Polyurethane Scaffolds and Fibrin Hydrogels. J. Tissue Eng. Regen. Med 2016, 10, E409–E418 [PubMed: 24170732]

(16). Li B; Davidson JM; Guelcher SA The Effect of the Local Delivery of Platelet-Derived Growth Factor from Reactive Two-Component Polyurethane Scaffolds on the Healing in Rat Skin Excisional Wounds. Biomaterials 2009, 30, 3486–3494. [PubMed: 19328544]

(17). Ma Z; Hong Y; Nelson DM; Pichamuthu JE; Leeson CE; Wagner WR Biodegradable Polyurethane Ureas with Variable Polyester or Polycarbonate Soft Segments: Effects of Crystallinity, Molecular Weight, and Composition on Mechanical Properties. Biomacromolecules 2011, 12, 3265–3274. [PubMed: 21755999]

(18). Caracciolo P; Buffa F; Abraham G Effect of the Hard Segment Chemistry and Structure on the Thermal and Mechanical Properties of Novel Biomedical Segmented Poly(ester urethanes).J. Mater. Sci. Mater. Med 2009,20, 145–155. [PubMed: 18704646]

(19). Guelcher SA; Gallagher KM; Didier JE; Klinedinst DB; Doctor JS; Goldstein AS; Wilkes GL; Beckman EJ; Hollinger JO Synthesis of Biocompatible Segmented Polyurethanes from Aliphatic Diisocyanates and Diurea Diol Chain Extenders. Acta Biomater. 2005, 1, 471–484. [PubMed: 16701828]

(20). Guan J; Sacks MS; Beckman EJ; Wagner WR Biodegradable Poly(ether ester urethane)urea Elastomers Based on Poly(ether ester) Triblock Copolymers and Putrescine: Synthesis, Characterization and Cytocompatibility. Biomaterials 2004, 25, 85–96. [PubMed: 14580912]

(21). Thijs HM; Becer CR; Guerrero-Sanchez C; Fournier D; Hoogenboom R; Schubert US Water Uptake of Hydrophilic Polymers Determined by a Thermal Gravimetric Analyzer with a Controlled Humidity Chamber. J. Mater. Chem 2007, 17, 4864–4871.

(22). Alomayri T; Assaedi H; Shaikh F; Low IM Effect of Water Absorption on the Mechanical Properties of Cotton Fabric-Reinforced Geopolymer Composites. J. Asian Ceram. Soc 2014, 2, 223–230.

(23). Musto P; Ragosta G; Scarinzi G; Mascia L Probing the Molecular Interactions in the Diffusion of Water through Epoxy and Epoxy–Bismaleimide Networks J. Polym. Sci. Part B: Polym. Phys 2002, 40, 922–938.

(24). Bogdanov B; Vidts A; Van Den Buicke A; Verbeeck R; Schacht E Synthesis and Thermal Properties of Poly(ethylene glycol)-Poly(ε-caprolactone) Copolymers. Polymer 1998, 39, 1631–1636.

(25). Xu C; Huang Y; Wu J; Tang L; Hong Y Triggerable Degradation of Polyurethanes for Tissue Engineering Applications. ACS Appl. Mater. Interfaces 2015, 7, 20377–20388. [PubMed: 26312436]

(26). Hong Y; Guan J; Fujimoto KL; Hashizume R; Pelinescu AL; Wagner WR Tailoring the Degradation Kinetics of Poly(ester carbonate urethane)urea Thermoplastic Elastomers for Tissue Engineering Scaffolds. Biomaterials 2010, 31, 4249–4258. [PubMed: 20188411]

(27). Asplund JB; Bowden T; Mathisen T; Hilborn J Synthesis of Highly Elastic Biodegradable Poly(urethane urea). Biomacromolecules 2007, 8, 905–911. [PubMed: 17263577]

(28). Xu C; Yepez G; Wei Z; Liu F; Bugarin A; Hong Y Synthesis and Characterization of Conductive, Biodegradable, Elastomeric Polyurethanes for Biomedical Applications. J. Biomed. Mater. Res., A 2016, 104, 2305–2314. [PubMed: 27124702]

(29). Guan J; Fujimoto KL; Sacks MS; Wagner WR Preparation and Characterization of Highly Porous, Biodegradable Polyurethane Scaffolds for Soft Tissue Applications. Biomaterials 2005, 26, 3961–3971. [PubMed: 15626443]

(30). Zhang R; Ma PX Poly(alpha-hydroxyl acids)/Hydroxyapatite Porous Composites for Bone-Tissue Engineering. I. Preparation and Morphology. J. Biomed. Mater. Res 1999, 44, 446–455. [PubMed: 10397949]

(31). Hsu YY; Gresser JD; Trantolo DJ; Lyons CM; Gangadharam PR; Wise DL Effect of Polymer Foam Morphology and Density on Kinetics of *In Vitro* Controlled Release of Isoniazid from Compressed Foam Matrices. J. Biomed. Mater. Res 1997, 35, 107–116. [PubMed: 9104703]

(32). Punnakitikashem P; Truong D; Menon JU; Nguyen KT; Hong Y Electrospun Biodegradable Elastic Polyurethane Scaffolds with Dipyridamole Release for Small Diameter Vascular Grafts. Acta Biomater.2014, 10, 4618–4628. [PubMed: 25110284]

(33). Delpech MC; Miranda GS Waterborne Polyurethanes: Influence of Chain Extender in FTIR Spectra Profiles. Cent. Eur. J. Eng 2012, 2, 231–238.

(34). Wang F; Li Z; Lannutti JL; Wagner WR; Guan J, Synthesis, Characterization and Surface Modification of Low Moduli Poly(ether carbonate urethane) ureas for Soft Tissue Engineering. Acta Biomater. 2009, 5, 2901–2912. [PubMed: 19433136]

(35). Korley LTJ; Pate BD; Thomas EL; Hammond PT Effect of the Degree of Soft and Hard Segment Ordering on the Morphology and Mechanical Behavior of Semicrystalline Segmented Polyurethanes. Polymer 2006, 47, 3073–3082.

(36). Spaans C; De Groot J; Dekens F; Pennings A High Molecular Weight Polyurethanes and a Polyurethane Urea Based on 1, 4-Butanediisocyanate. Polym. Bull. 1998, 41, 131–138.

(37). Storey RF; Hickey TP Degradable Polyurethane Networks based on D, L-lactide, Glycolide, epsilon-Caprolactone, and Trimethylene Carbonate Homopolyester and Copolyester Triols. Polymer 1994, 35, 830–838.

(38). Saad B; Matter S; Ciardelli G; Neuenschwander P; Suter U; Uhlschmid G; Welti M Interactions of Osteoblasts and Macrophages with Biodegradable and Highly Porous Polyesterurethane Foam and its Degradation Products. J. Biomed. Mater. Res 1996, 32, 355–366. [PubMed: 8897140]

(39). Cohn D; Stern T; GonzÃ¡lez MF; Epstein J Biodegradable Poly(ethylene oxide)/Poly (ε-caprolactone) Multiblock Copolymers. J. Biomed. Mater. Res 2002, 59, 273–281. [PubMed: 11745563]

(40). Yang C; Lin W; Liu F Waterborne Polyurethane Single-Ion Electrolyte from Aliphatic Diisocyanate and Various Molecular Length of Polyethylene Glycol. Express Polym. Lett 2007, 1, 142–149.

(41). Kloczkowski A Application of Statistical Mechanics to the Analysis of Various Physical Properties of Elastomeric Networks—A Review. Polymer 2002, 43, 1503–1525.

(42). Yiu C; King N; Pashley DH; Suh B; Carvalho R; Carrilho M; Tay F Effect of Resin Hydrophilicity and Water Storage on Resin Strength. Biomaterials 2004, 25, 5789–5796. [PubMed: 15147825]

(43). Charriere E; Lemaitre J; Zysset P Hydroxyapatite Cement Scaffolds with Controlled Macroporosity: Fabrication Protocol and Mechanical Properties. Biomaterials 2003, 24, 809–817. [PubMed: 12485799]

(44). Loh XJ; Tan KK; Li X; Li J The *In Vitro* Hydrolysis of Poly(ester urethane)s Consisting of Poly[(R)-3-hydroxybutyrate] and Poly(ethylene glycol). Biomaterials 2006, 27, 1841–1850. [PubMed: 16305807]

(45). Tokiwa Y; Suzuki T Hydrolysis of Polyesters by Lipases. Nature 1977, 270, 76–78. [PubMed: 927523]

(46). Kim YD; Kim SC Effect of Chemical Structure on the Biodegradation of Polyurethanes under Composting Conditions. Polym. Degrad. Stabil1998, 62, 343–352.

(47). Pringle JH; Fletcher M Influence of Substratum Wettability on Attachment of Freshwater Bacteria to Solid Surfaces. Appl. Environ. Microbiol 1983, 45, 811–817. [PubMed: 16346243]

(48). Gu JD; Yang S; Welton R; Eberiel D; McCarthy SP; Gross RA Effect of Environmental Parameters on the Degradability of Polymer Films in Laboratory-Scale Composting Reactors. J. Environ. Polym. Degrad 1994, 2, 129–135.

(49). Christenson EM; Patel S; Anderson JM; Hiltner A Enzymatic Degradation of Poly(ether urethane) and Poly(carbonate urethane) by Cholesterol Esterase. Biomaterials 2006, 27, 3920–3926. [PubMed: 16600363]

(50). Van Minnen B; Van Leeuwen M; Kors G; Zuidema J; Van Kooten T; Bos R In Vivo Resorption of a Biodegradable Polyurethane Foam, Based on 1, 4-Butanediisocyanate: A Three-Year Subcutaneous Implantation Study. J. Biomed. Mater. Res., A 2008, 85, 972–982. [PubMed: 17907243]

(51). Liao J; Yang L;Grashow J; Sacks MS Molecular Orientation of Collagen in Intact Planar Connective Tissues under Biaxial Stretch. Acta Biomater. 2005, 1, 45–54. [PubMed: 16701779]

(52). Freytes DO; Badylak SF; Webster TJ; Geddes LA; Rundell AE 2004.Biaxial Strength of Multilaminated Extracellular Matrix Scaffolds. Biomaterials 2004, 25, 2353–2361. [PubMed: 14741600]

(53). Huang Y; Ren J; Chen C; Ren T; Zhou X Preparation and Properties of Poly(lactide-co-glycolide) (PLGA)/Nano-Hydroxyapatite (NHA) Scaffolds by Thermally Induced Phase Separation and Rabbit MSCs Culture on Scaffolds. J. Biomater. Appl 2007, 22, 409–432. [PubMed: 17494961]

(54). Wei G; Ma PX Structure and Properties of Nano-Hydroxyapatite/Polymer Composite Scaffolds for Bone tissue Engineering. Biomaterials 2004, 25, 4749–4757. [PubMed: 15120521]

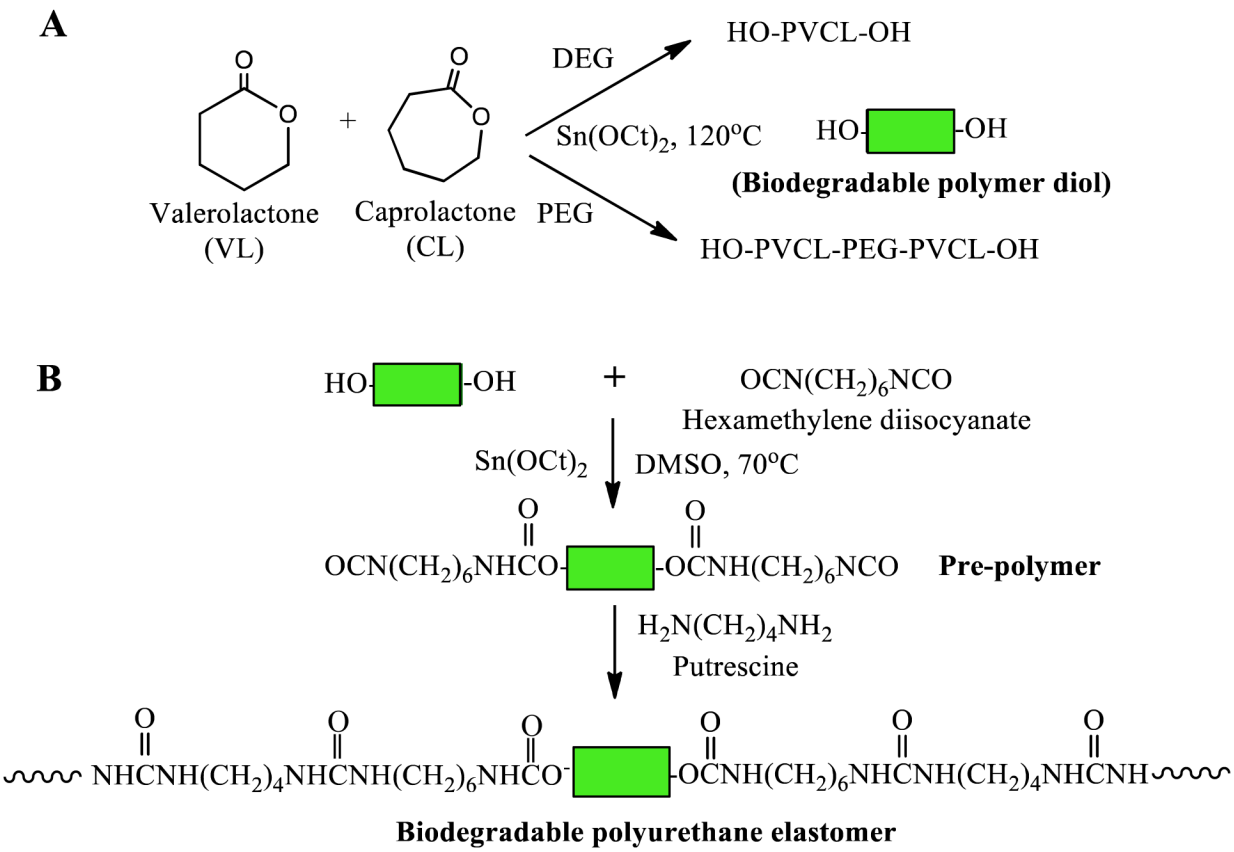

Figure 1.
Synthetic scheme of (A) PVCL or PVCL-PEG-PVCL copolymer diols and (B) polyurethanes.

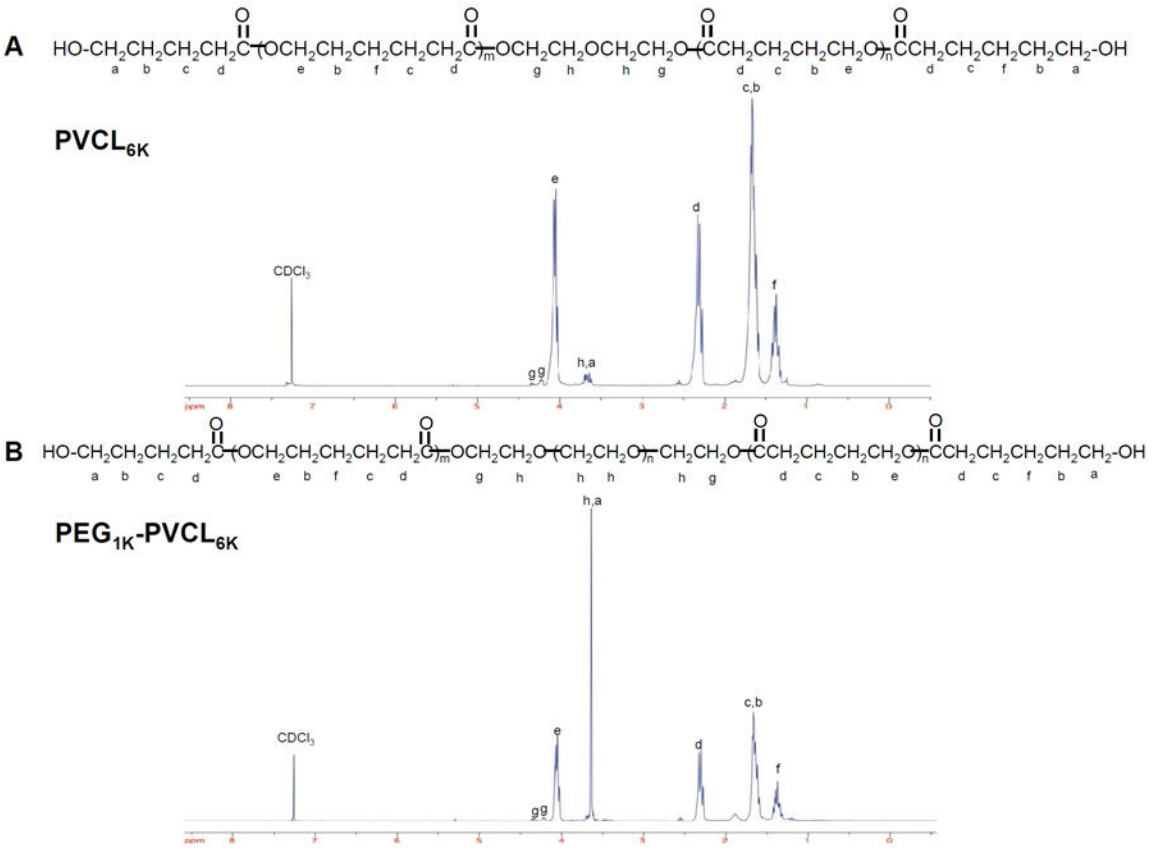

Figure 2.
^{1}H-NMR spectra of (A) PVCL and (B) PVCL-PEG-PVCL copolymer diols.

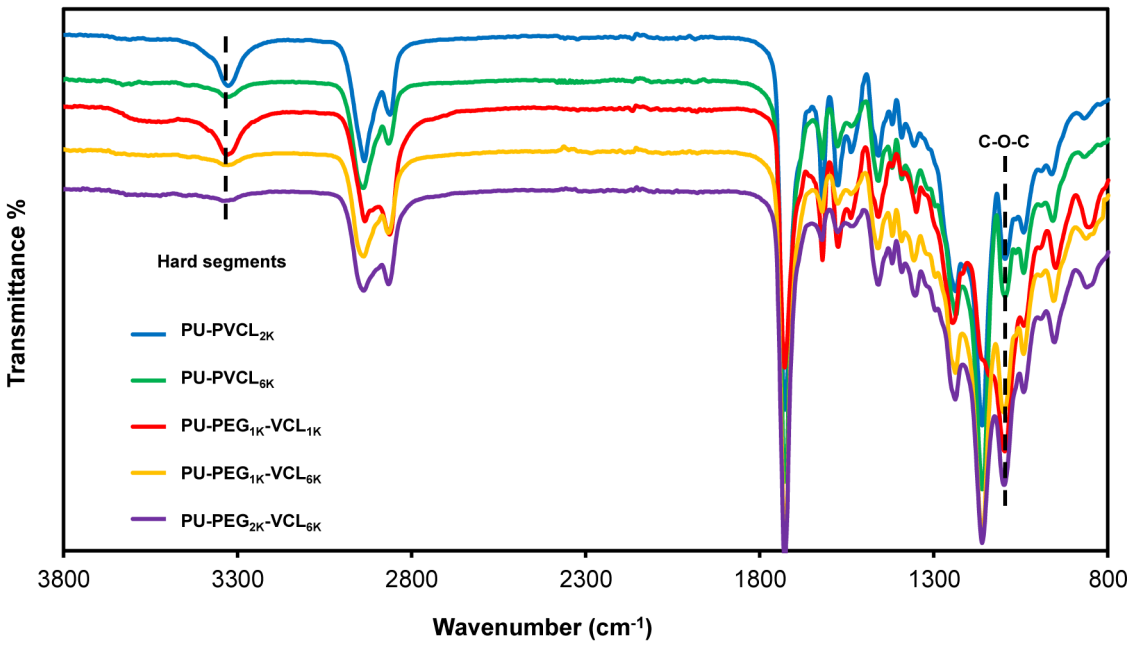

Figure 3.
FT-IR spectra of polyurethanes.

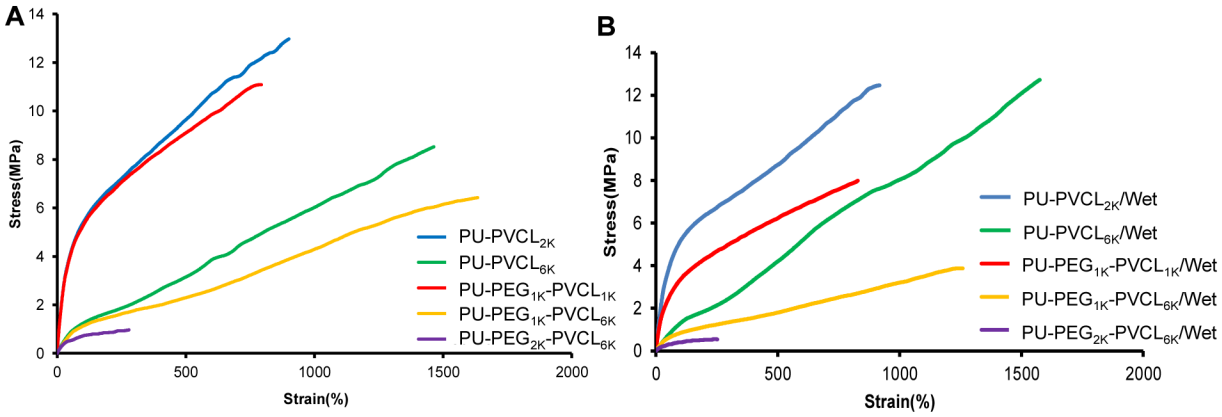

Figure 4.
Typical stress-strain curves of the polyurethane films in (A) dry and (B) wet states.

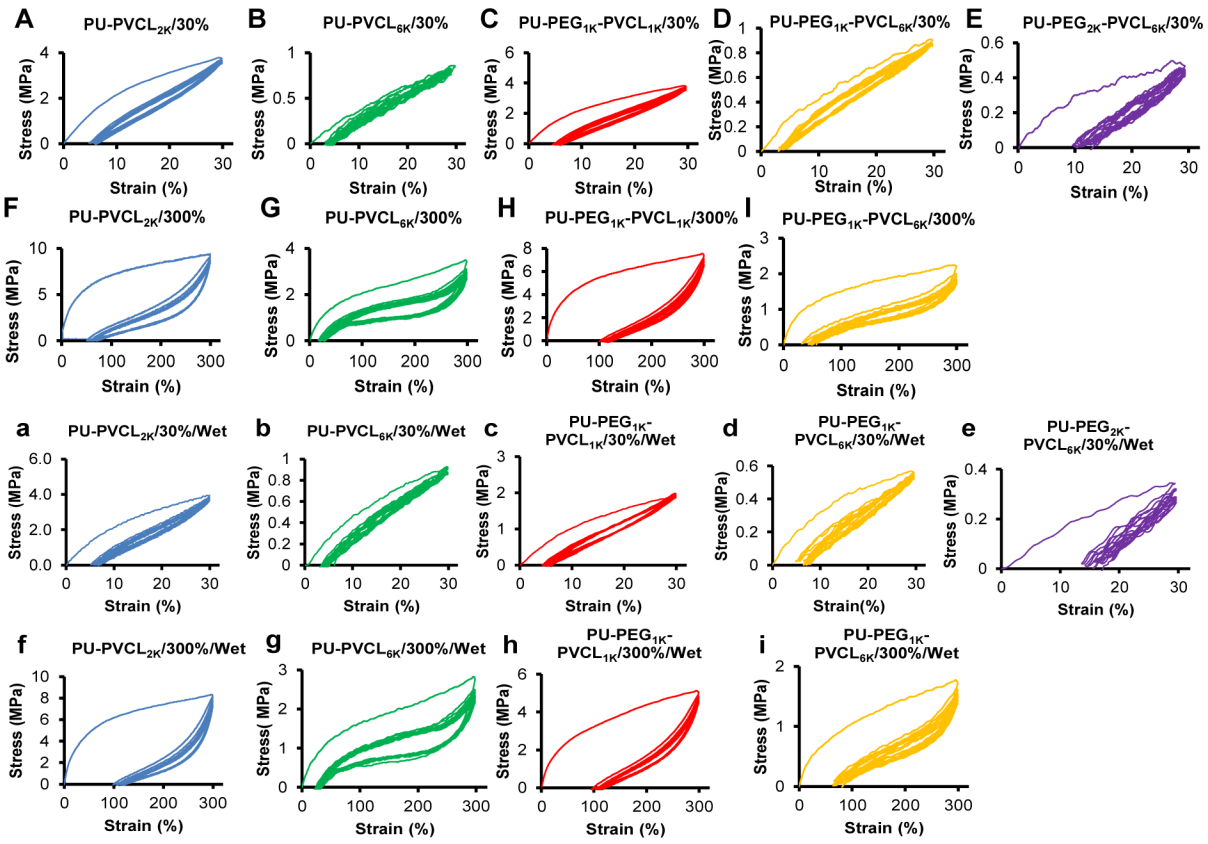

Figure 5.

Cyclic stretching of polyurethane films in dry state with 30% (A-E) and 300% (F-I) strains, and in wet state with 30% (a-e) and 300% (f-i) strains. The PU-PEG_{2K}-$PVCL_{6K}$ film is too week to obtain cyclic stretching curves at 300% deformation in both dry and wet states.

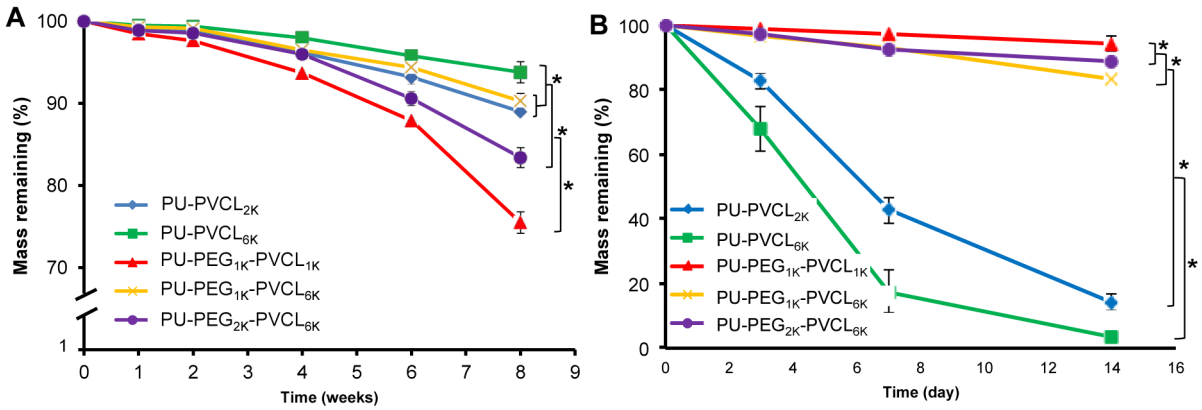

Figure 6.
Mass remaining for polyurethane films in (A) PBS and (B) 100 U/mL lipase/PBS at 37 °C.

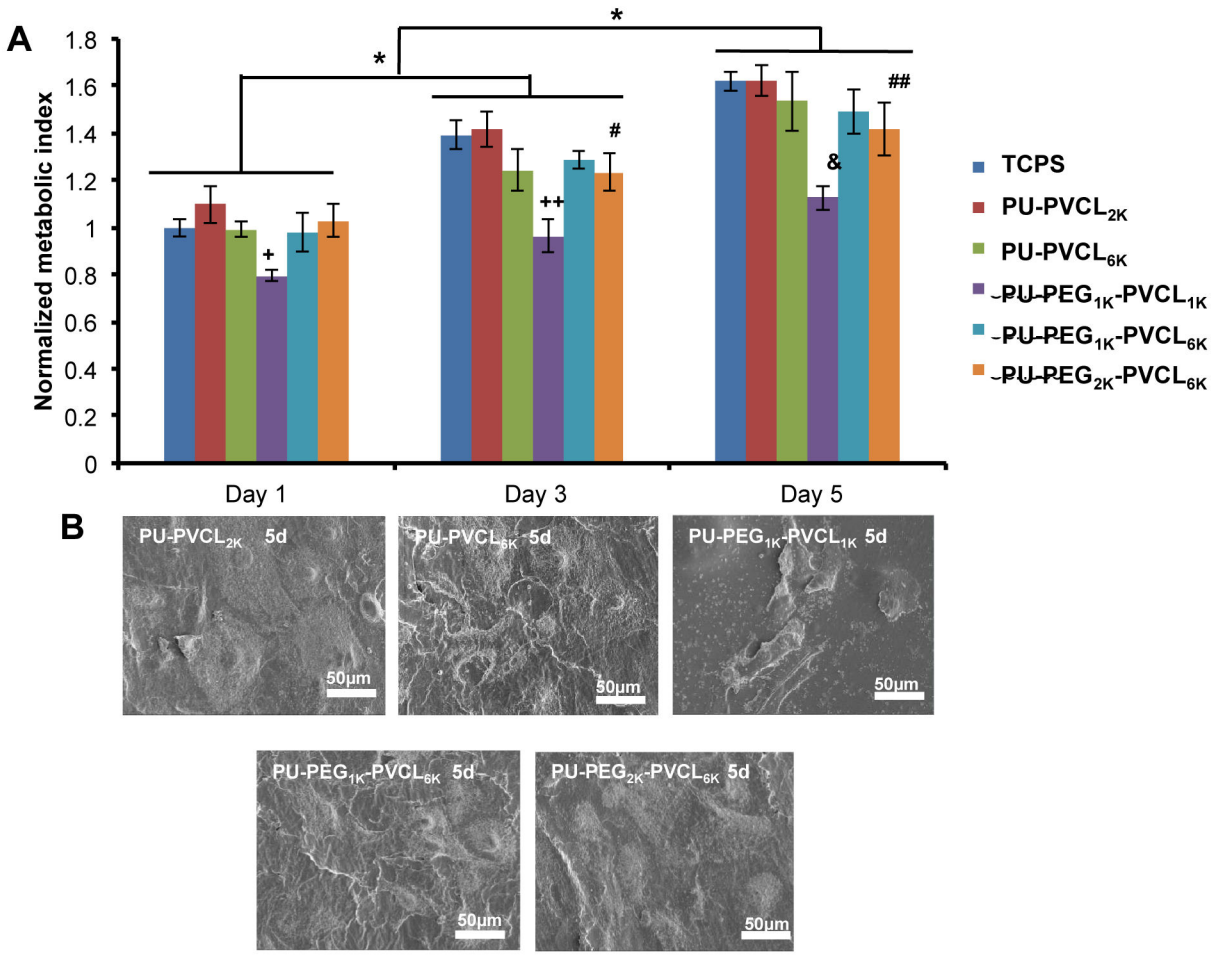

Figure 7.

Cell compatibility of polyurethane films. (A) Metabolic index of 3T3 fibroblasts cultured on polyurethane film surfaces. Tissue cultured polystyrene (TCPS) was a positive control. +: p<0.0003, PU-PEG$_{1K}$-PVCL$_{1K}$ compared to other groups at day 1. ++, &: p<0.0001, PU-PEG$_{1K}$-VCL$_{1K}$ compared with other groups at days 3 and 5, respectively. #,##:p<0.05, PU-PEG$_{2K}$-PVCL$_{6K}$ compared with TCPS, PU-PVCL$_{2K}$ and PU-PEG$_{1K}$-PVCL$_{1K}$ at days 3 and 5, respectively. (B) Electron micrographs of the PU-PEG-PVCL films seeded with 3T3 fibroblasts at 5 d.

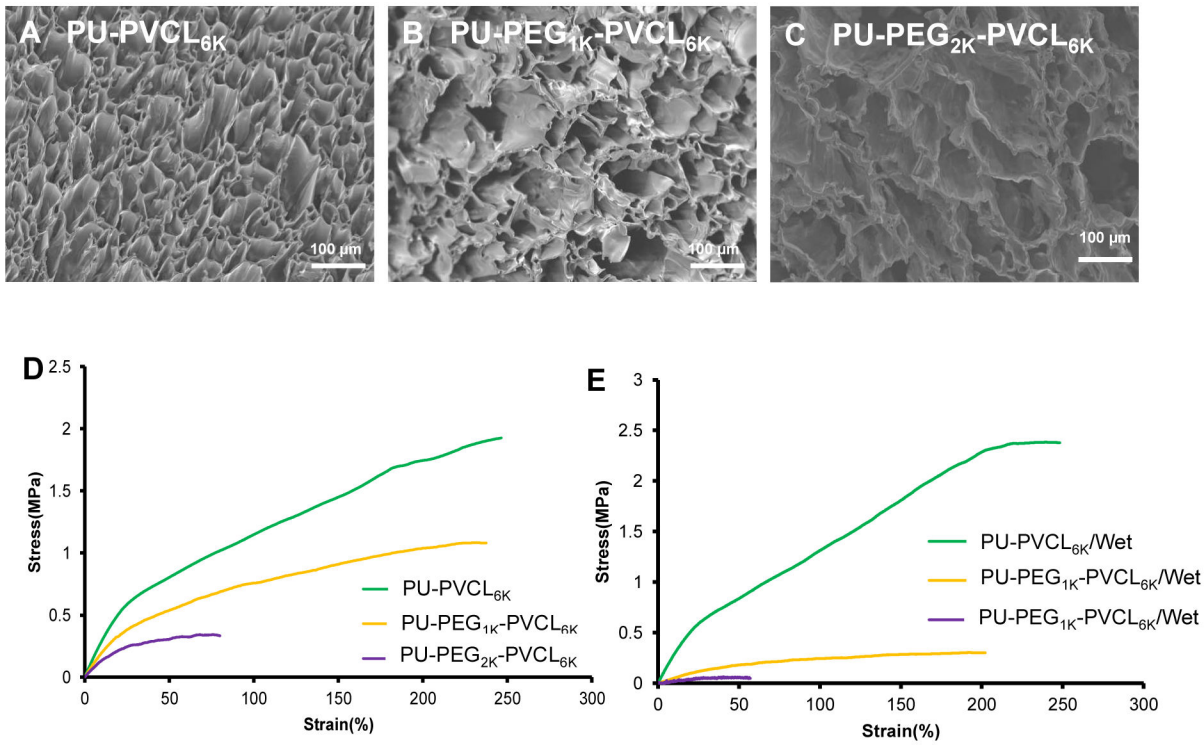

Figure 8.

Porous scaffold characterization. Electron micrographs of (A) PU-$PVCL_{6K}$, (B) PU-PEG_{1K}-$PVCL_{6K}$ and (C) PU-PEG_{2K}-$PVCL_{6K}$ porous scaffolds. Typical stress-strain curves of PU-$PVCL_{6K}$, PU-PEG_{1K}-$PVCL_{6K}$ and PU-PEG_{2K}-$PVCL_{6K}$ porous scaffolds in (D) dry and (E) wet states.

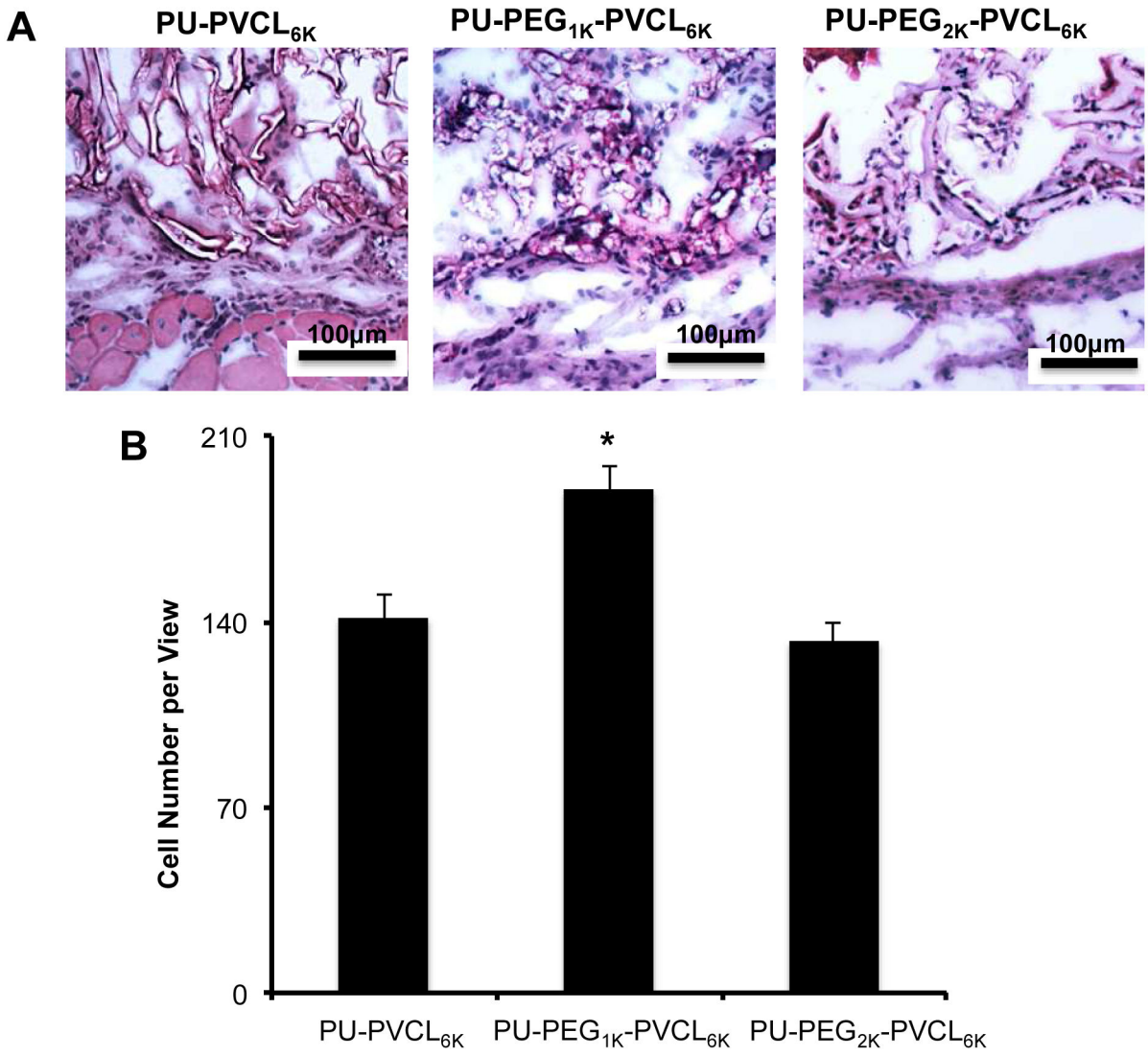

Figure 9.

Histological analysis of tissue responses to subcutaneous implanted scaffolds made of PU-$PVCL_{6K}$, PU-PEG_{1K}-VCL_{6K} or PU-PEG_{2K}-VCL_{6K}. (A) Representative images of H&E stains of implants and surrounding tissue at 2 weeks reveal mild inflammatory cell accumulation at the implant: tissue interface (200 × magnifications). A significant cell infiltration was also found inside all scaffolds. (B) Cell number per area on the implants was quantified and statistically analyzed with student's t-test (Mean ± SD. *p<0.05).

Table 1.

Block length of polyurethane soft segment

Polyurethane soft segment	Theoretical molar ratio of CL/VL	Calculated molar ratio of CL/VL	Theoretical block length of PVCL or PVCL-PEG-PVCL	Calculated block length of PVCL or PVCL-PEG-PVCL
$PVCL_{2K}$	50/50	58/42	2000	1936
$PVCL_{6K}$	50/50	53/47	6000	5576
PEG_{1K}-$PVCL_{1K}$	50/50	57/43	500-1000-500	493-1000-493
PEG_{1K}-$PVCL_{6K}$	50/50	51/49	3000-1000-3000	2763-1000-2763
PEG_{2K}-$PVCL_{6K}$	50/50	58/42	3000-2000-3000	2873-2000-2873

Table 2.

Polymer film characterization*

Samples	Tg (°C)	Tm (°C)	Inherent viscosity (dL/g)	Contact angle (°)	Water Absorption (%)	Tensile strength (MPa)		Initial modulus (MPa)		Breaking strain (%)		Instant recovery (%)
						Dry state	Wet state	Dry state	Wet state	Dry state	Wet state	
PU-PVCL$_{2K}$	−59	9	1.42	65±4^{a}	24±2^{a}	14.4±1.8^{a}	13.4±1.5^{a}	17.3±1.9^{a}	16.7±1.5^{a}	1212±245^{a}	1050±178^{a}	99±1
PU-PVCL$_{6K}$	−64	6	1.98	79±5^{b}	12±3^{b}	10.6±1.7^{a}	13.3±0.9^{a}	3.1±0.6^{b}	3.8±0.5^{b}	1588±65^{b}	1785±165^{b}	100±1
PU-PEG$_{1K}$-PVCL$_{1K}$	−63	−7	1.49	28±3^{c}	65±5^{c}	12.2±1.3^{a}	8.2±0.9^{b}	18.6±0.7^{a}	9.1±0.5^{c}	855±204^{c}	808±60^{a}	100±1
PU-PEG$_{1K}$-PVCL$_{6K}$	−66	7	2.05	69±2^{a,d}	23±3^{a}	6.4±0.4^{b}	4.3±0.3^{c}	3.5±0.4^{b}	2.3±0.6^{d}	1629±249^{b}	1470±229^{c}	100±2
PU-PEG$_{2K}$-PVCL$_{6K}$	−67	8	2.17	61±3^{a,e}	41±7^{d}	1.1±0.2^{c}	0.7±0.1^{d}	2.2±0.3^{b}	0.9±0.3^{e}	296±59^{d}	244±35^{d}	99±1

**a, b, c, d, and e* denote significantly difference for each group and each characteristic.

Table 3.

Scaffold characterization *

Samples	Porosity (%)	Pore size (μm)	Tensile strength (MPa)		Initial modulus (MPa)		Strain at peak stress (%)		Instant recovery (%)
			Dry state	Wet state	Dry state	Wet state	Dry state	Wet state	
PU-PVCL$_{6K}$	90±2	58±34	2.13±0.20^{a}	2.50±0.36^{a}	3.14±0.52^{a}	3.47±0.24^{a}	219±24^{a}	250±13^{a}	100±1
PU-PEG$_{1K}$-PVCL$_{6K}$	93±2	54±26	1.08±0.16^{b}	0.31±0.03^{b}	1.91±0.13^{b}	0.60±0.14^{b}	253±13^{a}	209±36^{a}	100±1
PU-PEG$_{2K}$-PVCL$_{6K}$	94±3	64±39	0.42±0.05^{c}	0.07±0.01^{c}	1.19±0.33^{c}	0.19±0.08^{c}	82±25^{b}	91±32^{b}	98±1

*a, b, and c denote significantly difference for each group and each characteristic.